Dynamic Stress Chain Formation in a Two-dimensional Particle Bed

by Keith M. Roessig, Joseph C. Foster, Jr., and Scott G. Bardenhagen

ABSTRACT—Cure cast plastic bonded explosives (PBXs) consist of relatively hard particles in a soft binder. Under compressive loading, the explosive crystals come into contact that causes high stress concentrations. The lines along which the crystals are loaded are called stress chains. Damage done to these particle beds during compressive loading can lead to reaction. The photoelastic effect of PMMA is exploited to examine the stress state within a two-dimensional particle bed. Stress chain development within the bed is recorded and is shown to increase the stress state within some particles while leaving others unloaded. These concentrations form early in the loading process, leading to fracture along the stress bridges and generating likely reaction initiation sites. Through material point method simulations, contact friction is shown to have a large effect on the stress distribution within the particle bed.

KEY WORDS—Stress chain, stress bridging, particulate materials, photoelasticity, material point method

Introduction

Many modern energetic materials consist of explosive crystals in a plasticized binder. These materials are much less sensitive than the pure explosive, but are subjected to a much wider range of mechanical loading conditions. As opposed to shock loading with pressures on the order of 1-5 GPa for up to a microsecond, these materials can be subjected to a mechanical loading with 100-500 MPa pressures for up to a millisecond. With the addition of shear deformation within the explosive crystals, conditions are such that reaction can occur. Understanding the conditions in which this reaction leads to sympathetic detonation is critical in the safe and economical use of energetic materials.

Particulate material behavior is of interest in examining phenomena from granular flow in soils to bonded particles in concrete and geologic formations,[1,2] but the failure of the crystals within the particle bed takes on a much more important role in cast-cure explosives. These materials generally consist of particles approximately 100-200 μm in diameter surrounded by a soft binder. The binder has a very low strength and behaves viscoelastically. Stress distributions within these particulate materials are complicated; loads are concentrated in small areas and are not evenly distributed throughout the material as in the case of a continuum. The paths along which the load is supported are called stress chains or stress bridges. Under these conditions, certain particles support a large part of the load while others support no load at all. It has been postulated that stress chains form within the explosive particle bed during loading.[3] Increased stress along these paths leads to localized fracture and subsequent friction of newly formed surfaces, which is a possible source of hot spot formation within the explosive.[4]

Unconfined impact experiments on cure cast plastic bonded explosives (PBX) have been conducted at the Advanced Warhead Experimentation Facility of the Air Force Research Laboratory's Munitions Directorate located at Eglin AFB, Florida.[5,6] These tests consisted of impacting two cylindrical rods of material in a modified Taylor anvil test and revealed dynamic stress-strain data. These tests also allowed for post mortem examination of the crystal bed after impact. Figure 1 shows the undamaged mesoscale structure of an HMX based explosive and the fracture surface of a damaged piece of the same material. The scanning electron microscopy (SEM) image of the undamaged material shows crystals with rounded corners with sizes ranging from about 100-300 μm. The smaller round objects between the HMX crystals are aluminum particles. The damaged material shows many fracture surfaces. These are all internal surfaces where friction could also play a large role in a heating process. The cross section of the post test specimen in Fig. 2 is also from SEM, but the backscatter technique is used. This method shows contrast between molecular weights of the materials. The aluminum particles are a bright white while the explosive crystals are a gray color. The damage in this image is shown not to be evenly distributed. General damage of all crystals is not observed; there are distinct paths along which fracture has occurred. Cracks proceed directly through some crystals while others nearby are completely undamaged.

Unfortunately, post test examination does not reveal how the stress is distributed during the loading event. The stress bridges may form very late in the response after particle motion occurs and not have any role in the initiation of the material. Viscoplastic heating from shear deformation could be an alternate explanation in this case.[7] If the stress bridges form early, the particles can then be exposed to increased stress concentrations leading to crystal fracture. Using current experimental methods, it is very difficult, if not impossible, to examine the internal deformation at the mesoscale of the explosive during a dynamic event.[8] The magnitude of the length and time scales involved with dynamic testing of real explosives push the limits of current experimental techniques to observe the mesoscale response. In addition, there are

Keith M. Roessig is a PhD and Joseph C. Foster, Jr. is a PhD, Air Force Research Laboratory/Munitions Directorate, Eglin AFB, FL 32542-6810, USA. Scott G. Bardenhagen is a PhD, University of Utah, Mechanical Engineering Department, Salt Lake City, Utah 84112-9208, USA.

Original manuscript submitted: December 10, 2001.
Final manuscript received: May 15, 2002.

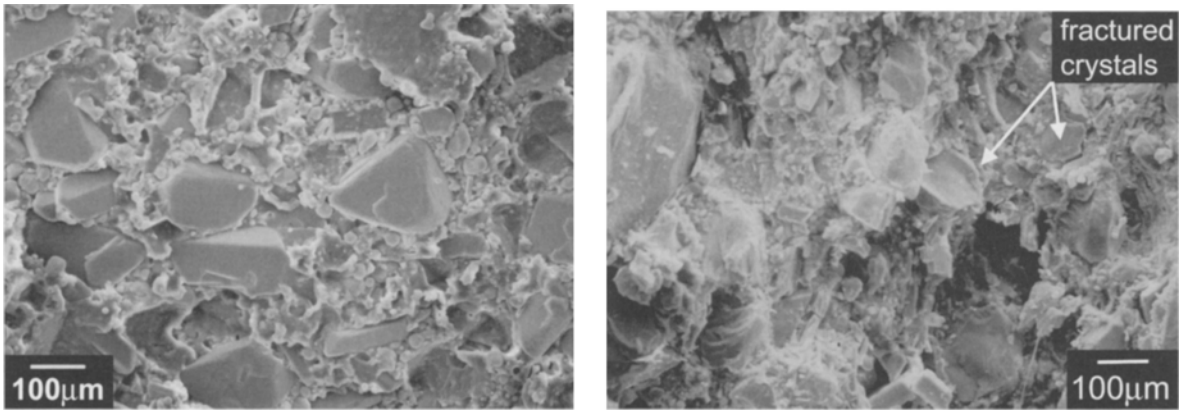

(a) (b)

Fig. 1—The undamaged specimen on the left shows HMX crystals with rounded edges. The specimen on the right shows damaged crystals from an unconfined impact test. The damaged crystals have sharp edges and exposed surfaces that are in contact with other crystals, allowing for internal friction under shearing deformation.

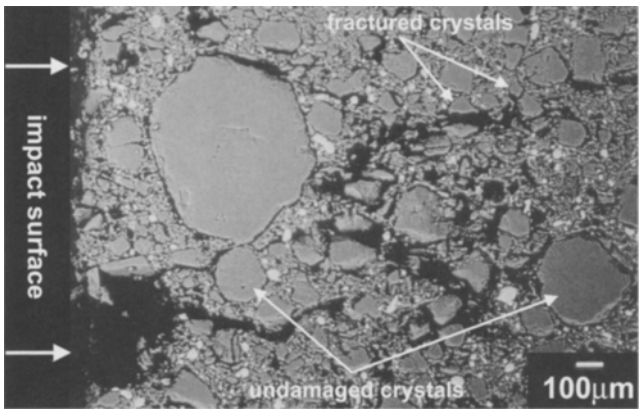

Fig. 2—The cross section of a cure cast plastic bonded explosive demonstrates the stress chain damage evolution within these types of particulate materials

numerous safety hazards in working with energetic materials. Therefore, it is necessary to create a different test to examine the contact mechanics and dynamic behavior of a particulate material subjected to mechanical loading.

Dynamic photoelasticity has been used to study the wave propagation through particulate materials. The dynamic load transfer through granular materials has been studied[9–11] as well as the effect of pulse length, wave velocity, and particle shape effects on the contact stresses.[12–14] The photoelastic method for predicting contact loads in dynamic experiments was validated by combining strain gage measurements with photoelastic measurements.[15,16] Photoelasticity has also been applied to study stress distributions in other situations including porous media,[17] cemented particles,[2,18] and crack propagation in finite sized specimens[19] and bimaterial interfaces.[20,21]

The photoelastic effect is exploited in this work to examine stress bridging in a simulated particulate material. Stress chains have not been observed in the particulate material studies mentioned above due to the loading conditions and the geometry of the experiments.

Procedures

In this effort, the photoelastic effect is used in conjunction with static and dynamic loading techniques to examine the response of a particulate material. A plane stress loading condition is developed by placing 6 mm thick discs within a loading frame described below. Static tests are performed on an Instron 1332 tension compression machine while the dynamic tests are completed on a 50 mm diameter split-Hopkinson compression bar.

Two materials were initially used in this work to simulate the explosive crystals: polymethylmethacrylate (PMMA) and polycarbonate (PC). PMMA was chosen as the only material for a number of reasons. PMMA was easily obtained in cast sheet, making manufacturing of the discs much less time consuming. PC sheet exhibited highly anisotropic properties due to the rolling operation performed during manufacturing. Though PC is much more optically sensitive, the experimental fringe patterns could not be reproduced due to anisotropy. Additionally, as the discs were taken to large stress levels prior to fracture, PC fringe patterns could not be resolved due to the abundance of fringes while PMMA produced a much more reasonable number of fringes for analysis. However, PMMA does exhibit viscoelastic behavior, and this is important in interpreting the results.

Loading Cell

The loading cell for both the static and dynamic tests consisted of a 4140 steel frame with adjustable sides that allowed for changes in width. Tests could then be run on a single line of discs in a "one-dimensional" configuration or in a two-dimensional planar array of discs. The top and bottom edges of the steel frame had 1.6 mm square notches machined every 3.2 mm. The side pieces had square teeth machined at the end to fit the notches of the top and bottom pieces. In this way, symmetric changes in width of the frame could be made every 6.4 mm. Grooves were machined into the interior sides of the pieces for additional support of the discs within the frame. A slot on the top piece allowed for a 6.4 mm thick loading pin to be inserted into the frame.

Static loading tests were conducted on an Instron 1332 tension/compression loading machine at a rate of 75 N/s. This gives an average strain rate of 1.5×10^{-4} s^{-1}. Dynamic tests were conducted by placing the load frame into a compression Hopkinson bar apparatus. The loading pulse could then be controlled by striker bar length and velocity and be recorded with digital oscilloscopes.

Photoelasticity

The photoelastic effect takes advantage of the fact that certain materials, when loaded, will cause light to propagate through them at different speeds along two perpendicular axes. This is called birefringence. Placing polarizers on each side of the specimen will generate interference patterns that depend on the types and positions of the polarizers. The configuration used in this work is called a circular polariscope. By using a combination of linear and quarter-wave polarizers on each side of the specimen, fringe patterns that follow lines of constant maximum shear stress are obtained. By calibrating these patterns with a known stress field, a photoelastic constant for the material can be determined for use in a wide variety of stress states. Complete discussion of the theory and applications of photoelasticity can be found by Dally and Riley[22] and Lee.[23]

Theoretical fringe patterns can be determined by generating the stress field within the specimen and then calculating the maximum shear stress at each point. Creating a contour plot of the maximum shear stress field generates the proper fringes once the photoelastic constant is determined from a known stress field. For the geometry used here, the elastic solution for a point load on a disc is used.[24] Following the method of Sienkiwicz *et al.*,[2] the stress for a point load can be superposed to generate the stress state for a distributed load. While the method used by Sienkiwicz *et al.* is used only for a pair of diametrically opposed pair of loads, it can be generalized using the same solution for a point load. One can rotate the point of application around the circle by an angle ϕ distributed over a contact zone of half width α, shown in Fig. 3. The stress equations for Cartesian coordinates become

$$\sigma_{xx} = \int_{-\alpha}^{\alpha} \left(\frac{2p(\beta)}{\pi} \frac{\sin^2(\theta_1+\phi)\cos(\theta_1)}{r_1} + \frac{p(\beta)}{2\pi R}\cos(\beta) \right) R d\beta \tag{1}$$

$$\sigma_{yy} = \int_{-\alpha}^{\alpha} \left(\frac{2p(\beta)}{\pi} \frac{\cos^2(\theta_1+\phi)\cos(\theta_1)}{r_1} + \frac{p(\beta)}{2\pi R}\cos(\beta) \right) R d\beta \tag{2}$$

$$\tau_{xy} = \int_{-\alpha}^{\alpha} \left(\frac{2p(\beta)}{\pi} \frac{\cos(\theta_1+\phi)\sin(\theta_1+\phi)\cos(\theta_1)}{r_1} \right) R d\beta, \tag{3}$$

where p is the load per unit length at the integration point, and β is the integration variable over the contact area. The equations must be integrated for each contact load. The geometric variables r_1 and θ_1 are shown in Fig. 3 and given by

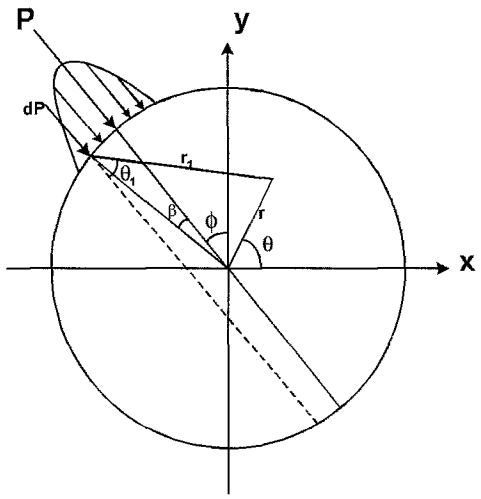

Fig. 3—Geometry and angle definitions for stress distribution determination for a Hertzian contact load on a circle

the relations

$$r_1 = \sqrt{r^2\cos^2(\theta-\phi-\beta) + \left(R - r\sin^2(\theta-\phi-\beta)\right)} \tag{4}$$

$$\theta_1 = \sin^{-1}\left(\frac{r\cos(\theta-\phi-\beta)}{r_1}\right). \tag{5}$$

A Hertzian load distribution is assumed[25] even though the discs are relatively thin. Any edge effects should be small and only affect the area immediate adjacent to the contact zone. The loading function p for the distributed forces along the contact zone is given by

$$p(\beta) = \frac{2P}{\pi R \sin\alpha}\sqrt{1 - \frac{\sin^2\beta}{\sin^2\alpha}} \tag{6}$$

where β is the integration variable over the contact zone and P is the total contact load. These equation are integrated for each contact load to determine total stress within the disc. From photoelasticity, the equation

$$\tau_{max} = \sqrt{\left(\frac{\sigma_{xx}-\sigma_{yy}}{2}\right) + \tau_{xy}^2} = \frac{Nf_\sigma}{2h} \tag{7}$$

is used to determine the fringe order across the entire disc. For the light field image used in these experiments, dark fringes occur when N is a multiple of $\frac{1}{2}$. A contour image of all the half order fringes will then predict the dark fringes photographed during the experiment. The variable f_σ is a material constant that must be measured with a calibrated test, and will vary depending upon wavelength of light used.

Results

Static Tests

The contours of maximum shear stress, described in a previous section, are generated using Matlab and superposed onto the original photograph of the disc. Figure 4 shows the

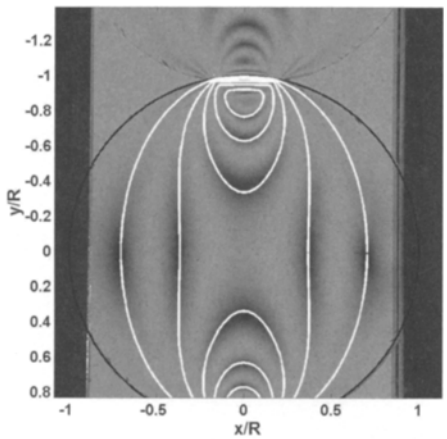

Fig. 4—Fringe patterns for a diametrical compression of 6700 N. R=2.54cm

white lines that are the mathematical contours and the dark regions that are experimentally generated fringes from a disc statically loaded at 6700 N. The figure also shows the disc immediately above to see the experimental contour lines without the superposed theoretical fringes. Contact zone length, which is very important to the stress distribution, is measured directly from the pictures. For static tests, the force is known from the load cell. Knowing the contact zone length and load allows fringe determination and therefore calibration of the photoelastic constant for the material.

The contours in Fig. 4 match very well except near the contact region where a three-dimensional stress state exists. The theoretical curves are also derived from linear elasticity, so a small deformation assumption exists. Near the contact zone, larger deformations distort the experimental contour field from the theoretical one, as seen in Fig. 5. At 8900 N, this effect is much more pronounced. At this load, the viscoelastic behavior of the material has caused large thickness changes, and therefore distortion in the fringe pattern, around the contact zone. Viscoelastic behavior and any plastic deformation can be verified by residual fringes after unloading.

The formation of stress bridges under static loading is shown in Fig. 6. Both loaded discs and unloaded discs appear in the particle bed, demonstrating that the load is not distributed evenly through the material. This is the same type of behavior seen in the damaged explosive in Fig. 2. Determining when these stress bridges form under dynamic loading is important to their possible role in mechanical initiation of energetic materials.

Dynamic Tests

A typical dynamic test is shown in Fig. 7. Both the full field and single discs with theoretical fringes are shown. The fringe patterns derived from the static elasticity solutions described in the *Photoelasticity* section match well with the dynamic fringe patterns. Though PMMA can exhibit viscoelastic properties, the initial loading of PMMA at this load rate has been shown to be linear until about 300 MPa at room temperature.[26] Therefore, once the disk has been loaded, the static, linear elastic solutions can predict the fringe patterns observed during dynamic loading.

The same geometry that produced stress chains in the static tests was used for the dynamic loading. The results of these tests can be seen in Fig. 8. The wave propagates along different paths, with the higher loads on the outer discs next to the steel frame. This is the same area that showed higher loads in the quasistatic loading shown in Fig. 6. The stress chains form with the initial wave impingement, indicating that stress chains establish themselves early in the loading process.

Discussion

The stress state of the particle bed consists of a symmetric pattern where there are two distinct paths on each half of the particle bed. The strong stress chains are positioned on the outer boundary while the weaker ones pass through the center. The two paths are labeled stronger and weaker due to the load levels within the two chains, known from the size and amount of the fringes within the disk. From Fig. 9, we can see that the bottom strong and weak stress chains are formed from the disks 1,5,10,14,18 and 1,2,7,11,15, respectively. By fitting contours to each of the discs at every frame, as shown in Fig. 7, the contact loads throughout the assembly can be determined. The time history of the loading between disks can be seen in Fig. 10. The cubic spline fits are intended for comparison of relative load levels and are not intended to convey quantitative information about the stress between the contact points. The dashed line is the spline fit for the final frame. The bottom strong stress chain load increases at the left and propagates to the right, then reflecting off the back edge. The final loading across the disks is fairly constant, showing a very long input stress pulse. The disks within the strong chain have approached a uniform stress state. The weak stress chain, however, does not see the increase in stress after wave reflection. The tendency for the dynamic stress state is to rapidly approach the static stress state, giving rise to stress concentrations early within the loading cycle. The possible measurement error in the load values of Fig. 10 is about a constant 250 N. The error percentage decreases with greater loads due to the larger number of fringes that occur and points per fringe that can be used to match theoretical and experimental fringe patterns. Error bars were not placed on Fig. 10 to prevent too much information being placed on the graph. These plots are intended to show general stress chain development, but not to determine exact stress concentrations.

The chains seem to have a large dependence on the boundary conditions. The strong stress chains form where waves impinging on the side supports reflect as compressive waves, increasing the overall load in the disk and resulting in more fringes. The loading is strengthened by the reflection at the back support, and the steady state is approached. This does not happen with the weaker chains, which occur in the interior of the particle bed. Experimental evidence of this type of behavior can be seen by the work of Boyle *et al.*[27] In those experiments, pressure/shear initiation of energetic materials was found to occur near the confinement walls. This is also where material point method simulations have shown the greatest amount of shear deformation.[28]

The contact mechanics of the problem determine the way in which the stress is distributed through the particle bed. Included in these mechanics are the materials properties of the constituents, contact geometry, and interfacial frictional properties. The friction between the particles determines the amount of shear deformation that can be transmitted between

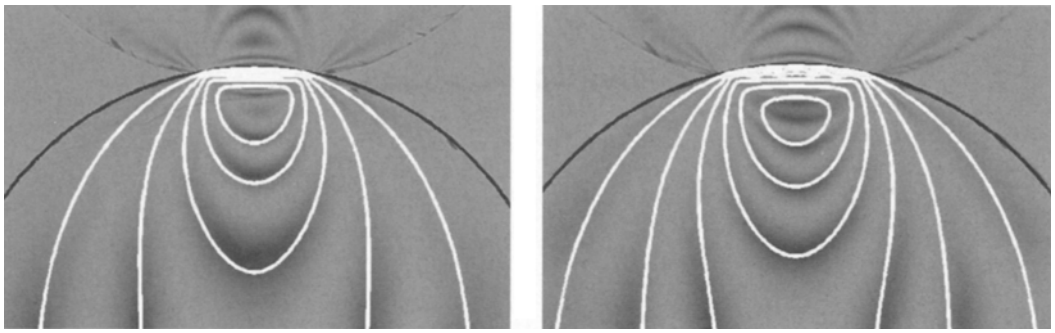

Fig. 5—Close view of the contact zone at loads of 6700 and 8900 N

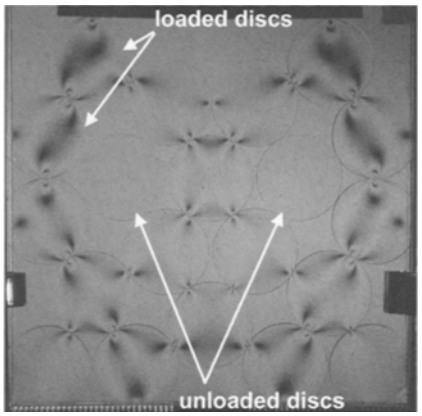

Fig. 6—Static stress chain development in PMMA discs. The load of 5500 N is not distributed evenly across the discs.

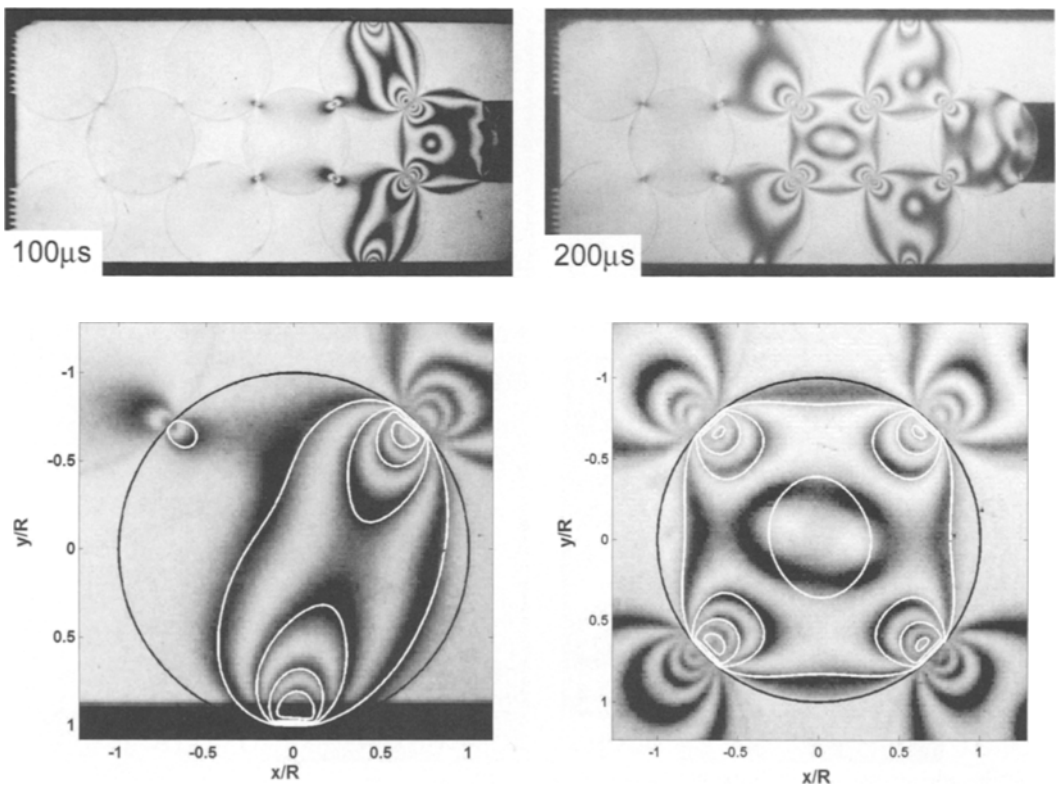

Fig. 7—Wave propagation in two dimensional array of PMMA discs and examples of mathematical contours generated in Matlab superposed on individual disks. R=2.54cm

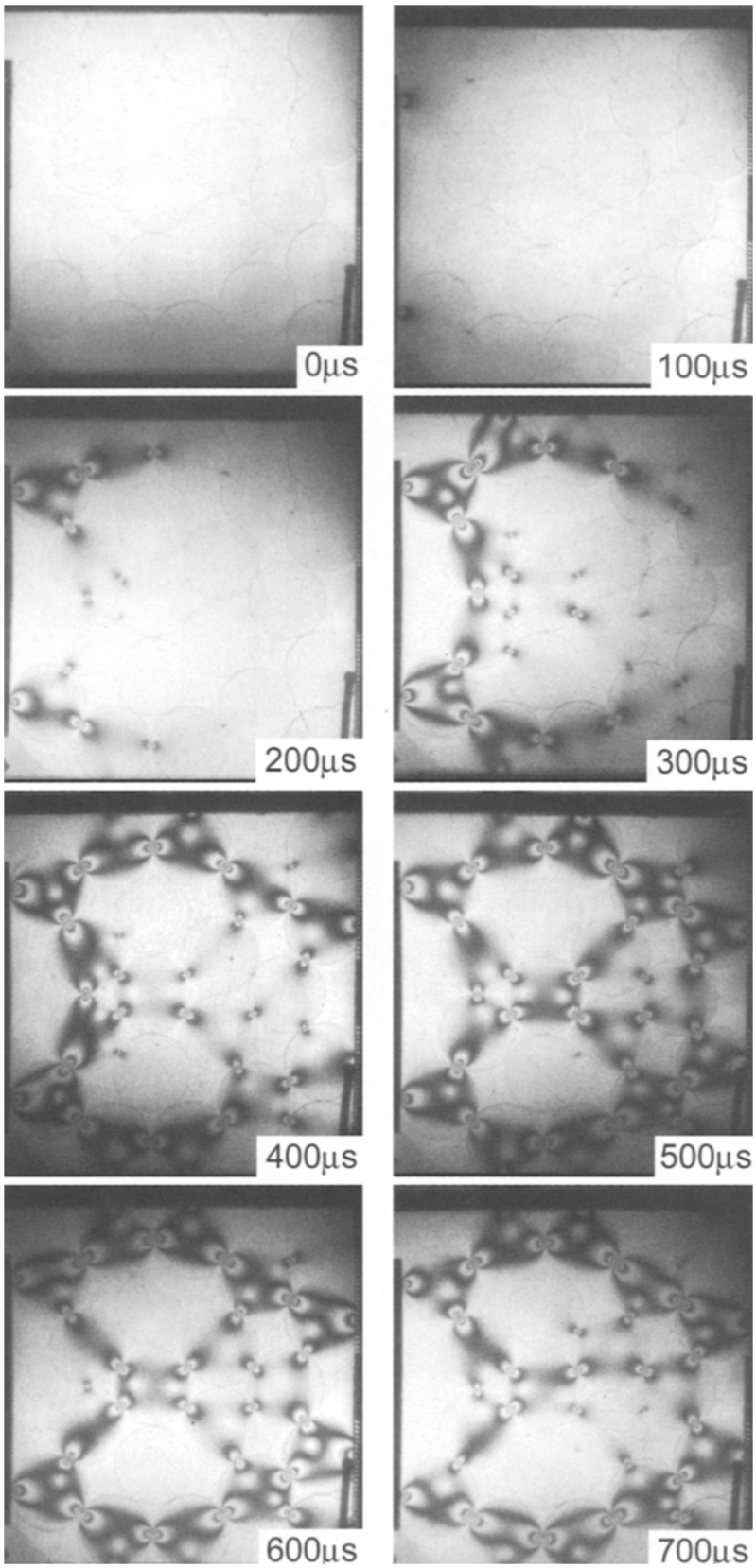

Fig. 8—Dynamic stress chain formation in two dimensional array of PMMA discs

Fig. 9—Disk numbers in the two dimensional stress chain geometry

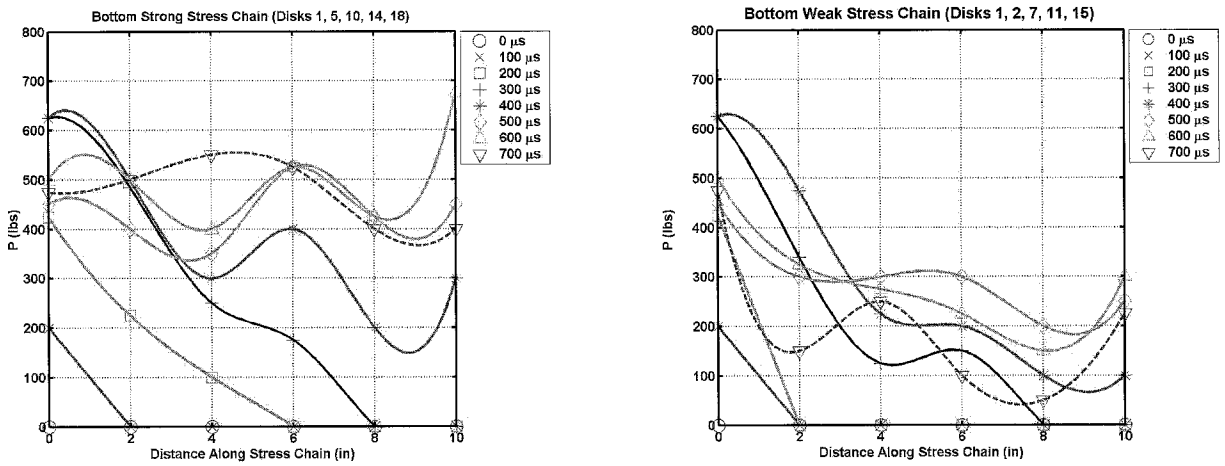

Fig. 10—Stress chain load levels for the bottom strong and weak chains

particles. Simulations of the experiment conducted here confirm the dependence. Figure 11 shows the half geometry of four separate simulations, each with a different friction coefficient. The first picture has a zero Coulomb friction condition, with the next view of 0.2 and 0.5 ending with a no slip condition. All of these pictures are views at the same point in time after the wave impinged the first disk. It is seen that the lower contact friction cases (0 or 0.2 coefficients) that reproduce the experimental results. The photoelastic technique used here was also used to examine the contact mechanics of a system with a binder.[29] Those experiments show a very diverse set of responses due solely to changes in the ability to transmit shear between the grains through the binder. Simulations by Bardenhagen *et al.*[30] also show the same results. In these particulate materials, the ability to transmit shear between grains directly reduces the stress concentrations within the bulk material. With the low frictional contact in this binderless experiment, which can also be thought of as a binder with a wave speed of zero, the greatest amount of stress increase due to geometrical concentrations is generated.

The actual stress level increases between a continuum and contact stresses in a particulate material will depend on the shape and position of the particles themselves. The circular disks used in this work are compared to squares with side lengths equal to the diameter of the circle. In this way, a stress increase in a single disc within a regularly spaced array is compared to a unit cell of a continuum. While this is a very simplified setup, it will give a first order approximation of the stress increases within a particulate material. Applying an 8900 N load on a 6.35 mm thick unit cell would give a stress of 27.5 MPa. The maximum equivalent stress generated using the Matlab routine on a circular particle with an equivalent load, but now distributed over a smaller area due to the contact geometry, is 141 MPa. This is five times greater than maximum equivalent stress for a continuum.

The contact geometry plays a large role in this analysis. Though circles are used here, real contact geometries will not be idealized. Due to the crystal structure of HMX or RDX, undamaged crystal shapes can include sharper edges as seen in Figs. 1 and 2. This will increase the stress intensities within the crystals as the shapes become more irregular. These stress concentrations are the areas likely for ignition.

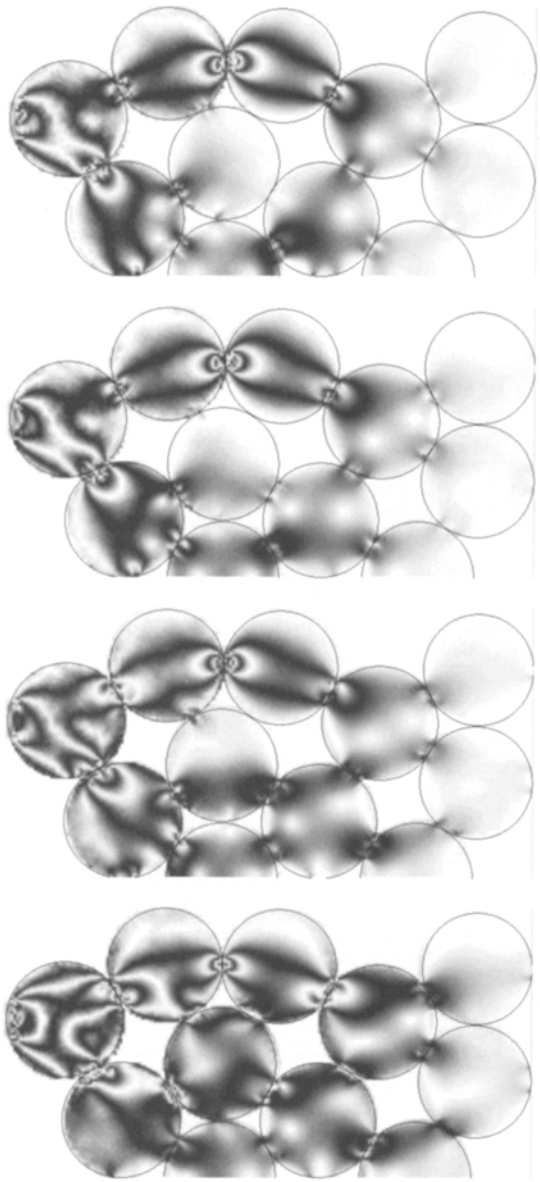

Fig. 11—Material-Point-Method simulations of the two dimensional stress chain geometry of PMMA discs. Four different frictional conditions are present: Coulomb friction coefficients, f, of 0, 0.2, 0.5 and a no-slip condition.

For a continuum, temperature increase and deformations for a distributed load are not enough to cause any appreciable reaction, certainly not one that could accelerate into a deflagration. Localized shear deformation within the crystals is needed to start a reaction.[31] As the equivalent stresses and shear deformations are concentrated into smaller regions, the effect is not negligible. Stress chains, and therefore deformation concentrations, occur early in the loading process and can be a viable method of mechanical initiation of energetic materials.

Conclusions

The photoelastic effect is used to examine the stress state within discs under planar compression, simulating the particulate nature of many cure cast plastic bonded explosives. The formation and subsequent fracture along stress concentrations known as stress chains within the materials is believed lead to reaction initiation sites.

PMMA discs are used to simulate an explosive crystal bed. Stress bridges formed under both static and dynamic loading. The stress chain that formed upon initial loading in the dynamic test was the same that formed in the static tests. The early formation of the stress bridge in the loading process confirms that it can localize deformation within the crystal bed. A first order approximation to the stress concentrations was shown to be approximately five times greater in the particulate material than for a continuum. Simulations of the experiment revealed that increased friction within this system allowed a load distribution across a greater percentage of particles.

Understanding this failure mode in this controlled environment is the first step to increasing the ability to predict the effect of mechanical insult upon the energetic materials of interest. Future homogenization of the mesoscale properties examined here will allow the determination of bulk mechanical material parameters that influence the macroscopic initiation behavior in the cure cast PBXs.

References

1. Haeger, H.M., Nagel, S.R., and Behringer, R.P. "The Physics of Granular Materials," Physics Today, **49** *(32) (1996).*

2. Sienkiwicz, F., Shukla, A., Sadd, M., Zhang, Z., and Dvorkin, J. "A Combined Experimental and Numerical Scheme for the Determination of Contact Loads Between Cemented Particles," Mechanics of Materials, **22** *(43), 43–50 (1996).*

3. Foster, J.C., Glenn, J.G., and Gunger, M. "Meso-scale Origins of the Low Pressure Equation of State and High Rate Mechanical Properties of Plastic Bonded Explosives." In Shock Compression in Condensed Matter—1999, M.D. Furnish, L.C. Chhabildas, and R.S. Hixson, eds., Proceedings of the Conference of the American Physical Society, pp. 703–706. Air Force Research Lab/Munitions Directorate (1999).

4. Davis, W.C. "High Explosives: The Interaction of Chemistry and Mechanics," Los Alamos Science, **2** *(1) (1981).*

5. Christopher, F.R., Jr., Foster, J.C., Wilson, L.L, and Gilland, H.L. "The Use of Impact Techniques to Characterize the High Rate Mechanical Properties of Plastic Bonded Explosives." In Proceeding of the 11th International Detonation Symposium, J.M. Short and J.E. Kennedy, eds. (1998).

6. Roessig, K.M., Foster, Jr., J.C., and Wilson, L.L. "High Strain Rate Behavior of Plastic Bonded Explosives." In Int. Workshop on New Models for Shock Wave/Dynamic Processes in Energetic Materials and Related Solids, S. Coffey, R. Armstrong, and V.Y. Klimenko, eds., University of Maryland (1999).

7. Ho, S.Y. "Impact ignition of rocket propellants," Combustion and Flame, **91**, *131–142 (1992).*

8. Rae, P.J., Goldrein, H.T., Palmer, S.J.P., and Proud, W. "Moire Interferometry Studies of pbx 9501," In Shock Compression of Condensed Matter—2001. AIP Conference Proceedings (2001).

9. Rossmanith, H.P. and Shukla, A. "Photoelastic Investigation of Dynamics Load Transfer in Granular Media," Acta Mechanica, **42** *(211) (1982).*

10. Shukla, A., Sadd, M.H., and Mei, H. "Experimental and Computational Modeling of Wave Propagation in Granular Materials," EXPERIMENTAL MECHANICS, **47** *(4), 377–381 (1990).*

11. Zhu, C.Y., Shukla, A., and Sadd, M.H. "Prediction of Dynamic Contact Loads in Granular Assemblies," J. Applied Mechanics, **58**, *341–346 (1991).*

12. Shukla, A., and Damania, C. "Experimental Investigation of Wave Velocity and Dynamic Contact Stresses in an Assembly of Disks," EXPERIMENTAL MECHANICS, **44** *(3), 268–281 (1987).*

13. Shukla, A., Sadd, M.H., Xu, Y., and Tai, Q.M. "Influence of Loading Pulse Duration on Dynamic Load Transfer in a Simulated Granular Medium," J. Mechanics and Physics of Solids, **41** *(1), 1795–1808 (1993).*

14. Shukla, A., Sadd, M.H., Singh, R., Tai, Q., and Vishwanathan, S. "Role of Particle Shape and Contact Profile on the Dynamic Response of Particulate Materials," Optics and Lasers in Engineering, **19** *(99) (1993).*

15. Xu, Y. and Shukla, A. "Evaluation of Static and Dynamic Contact Stresses in Simulated Granular Particles Using Strain Gages," J. Testing and Evaluation, **21** (3), 178–187 (1993).

16. Khanna, S.K. and Shukla, A. "On the Use of Strain Gages in Dynamic Fracture Mechanics," Engineering Fracture Mechanics, **51** (6), 933–948 (1995).

17. Shukla, A. and Prakash, V. "Wave Propagation in Porous Media as a Function of Fluid Saturation," EXPERIMENTAL MECHANICS, **47** (1), 80–87 (1990).

18. Sadd, M.H. and Shukla, A. "On the Role of Pore Fluid and Interparticle Cemenetation on Wave Propagation in Granular Materials," AMD-Vol. 188, Wave Propagation and Emerging Technologies, **188**, 11–28 (1994).

19. Zhu, C.Y., Chona, R., and Shukla, A. "Influence of Singularity Dominated Zone for Propagating Cracks in Finite Size Specimens," Theoretical and Applied Fracture Mechanics, **16**, 167–177 (1991).

20. Shukla, A. and Kavaturu, M. "Opening-mode Dominated Crack Growth Along Inclined Interfaces: Experimental Observations," Int. J. Solids and Structures, **35** (30), 3961–3975 (1998).

21. Signh, R., Lambros, J., Shukla, A., and Rosakis, A. "Investigation of the Mechanics of Intersonic Crack Propagation Along a Bimaterial Interface Using Coherent Gradient Sensing and Photoelasticity," Proc. R. Soc. Lond. A, **453**, 2649–2667 (1997).

22. Dally, J.W. and Riley, W.F., Experimental Stress Analysis. McGraw-Hill Book Company, New York (1965).

23. Lee, G.H. An Introduction to Experimental Stress Analysis. John Wiley & Sons, Inc., New York (1950).

24. Timoshenko, S. P. and Goodier, J. N. Theory of Elasticity. McGraw-Hill Book Company, New York, 3rd edition (1970).

25. Johnson, K. L. Contact Mechanics. Cambridge University Press, Cambridge, United Kingdom (1985).

26. Blumenthal, W.R., Cady, C.M., Lopez, M.F., Gray III, G.T., and Idar, D.J. "Influence of Temperature and Strain Rate on the Compressive Behavior of pmma and Polycarbonate Polymers." In Shock Compression of Condensed Matter—2001. AIP Conference Proceedings (2001).

27. Boyle, V., Frey, R., and Blake, O. Combined Pressure Shear Ignition of Explosives (1989).

28. Bardenhagen, S.G., Brackbill, J.U., and Sulsky, D. "Numerical Study of Stress Distribution in Sheared Granular Material in Two Dimensions," Physical Review E, **62** (3), 3882–3890 (2000).

29. Roessig, K.M. "Mesoscale Mechanics of Plastic Bonded Explosives." In Shock Compression of Condensed Matter—2001. AIP Conference Proceedings (2001).

30. Bardenhagen, S.G. and Brackbill, J.U. "Dynamic Stress Bridging in Granular Material," J. Applied Physics, **83** (11), 5732–5740 (1998).

31. Coffey, C.S. and Sharma, J. "Plastic Deformation, Energy Dissipation, and Initiation of Crystalline Explosives," Physical Review B, **60** (13), 9365–9371 (1999).